ACCELERATING SECTION FOR TECHNOLOGICAL ELECTRON LINAC

M.I. Ayzatsky, E.Z. Biller, A.N. Dovbnya, K.Yu. Kramarenko, I.V. Khodak, V.A. Kushnir, V.V. Mytrochenko, T.Ph. Nikitina, A.M. Opanasenko, S.A. Perezhogin, D.L. Stepin, L.I. Selivanov, V.Ph. Zhiglo
National Science Center "Kharkov Institute of Physics and Technology", Kharkov, Ukraine
E-mail: mitvic@kipt.kharkov.ua

The construction parameters and electrodynamic characteristics of the accelerating section with phase advance of 120° at the operating frequency of 2856 MHz are presented. This section is designed to upgrade the electron LINAC LU-10 at NSC KIPT. Experimental results are compared with calculated ones.

PACS: 29.20.Ej

INTRODUCTION

A powerful electron linac with beam energy of 10 MeV and average power up to 20 kW is under development at NSC KIPT. The linac gives the opportunity to accomplish both the scientific researches, in particular study of material properties for nuclear power plants, as well as the radiation processing.

Operating frequency and accelerating structure type were chosen based on the available technological facilities at NSC KIPT and the types of industrial klystrons (operating frequency is 2856 MHz, output pulse power is 5 MW and average power is to 36 kV). Accelerating structure is based on the cylindrical disk-loaded waveguide. A choice of the specific configuration of this waveguide is the results of simulations of section electrodynamic properties and beam dynamic characteristics [1].

The present paper is devoted to problems concerning fabrication and initial tuning of section cells, brazing of accelerating structure, vacuum testing, microwave measurements tuning of accelerating structure and. It should be noted that implementation of section tuning and microwave measurements requires the improving of the existing techniques with corresponding software and development of a new special equipment.

1. FABRICATION AND VACUUM TESTING

Fabrication of an accelerating section of resonance electron linac is rather complicated technological process that requires high qualified personals and special devices. Deep understanding of particle acceleration physics and of the undesirable consequences caused by some deviations in fabrication technology is the basis of this process.

It should be noted that each period of the linac sections developed and fabricated in NSC KIPT consists of ring and disk («disk-ring» technology). Sixteen ducts for coolant flow are located at the periphery of the disks and rings (Fig. 1) [2].

The whole section can be conventionally divided into two parts: travelling wave buncher (20 cells) and the main accelerating part (67 cells). To input and output the microwave power, there are two couplers at the entrance and exit of the accelerating section respectively. The travelling wave buncher parameters are significantly inhomogeneous. Such inhomogeneity is caused by the need of effective bunching: both the relative phase velocity β_{ph}, and the accelerating wave amplitude A should increase quite strongly (β_{ph} from 0.6 to 1 and A from 3.38 to 5.6 MV/m). To obtain the desired field amplitude distribution in the buncher, transition of iris radius from a = 16 mm to a = 14 mm is implemented using three diaphragms. As to the accelerating part, its geometrical dimensions vary quite smoothly in comparison with the buncher (change of iris radius is about 60 μm per cell).

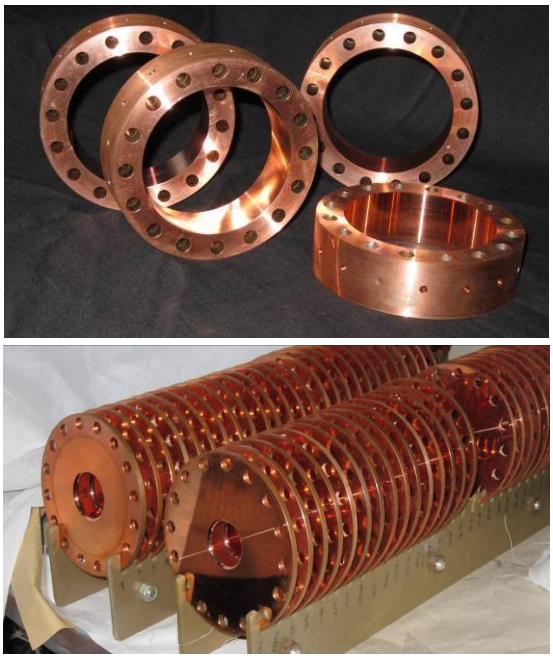

Fig. 1. Disks and rings of disk-loaded waveguide

In a first step of accelerating structure fabrication its separate elements, namely: disks and rings, were fabricated and preliminarily tuned. To realize the preliminarily tuning, rings are made with a tolerance on radius. The tuning is performed with special, so-called, π/2 cavity stack (Fig. 2) [3]. If we remove the central cells (cells are marked with a dashed line in Fig. 2) and combine the remaining parts, then we get the elementary stack consisting of three cells with three E_{010} mode resonance frequencies. These frequencies equal to the frequencies of 0, π/2 and π modes of periodic waveguide. Elementary stack is tuned so that π/2 mode frequency is equal to linac operating frequency with certain correction on vacuum, difference between tuning and operating temperature, braze influence and some frequency reserve to the final tuning, the results of which are re-

ported in the fourth section of this article. In stack central cell the amplitude of the longitudinal component of the electrical field intensity on the axis is zero at $\pi/2$ mode. Completely assembled cavity stack has six resonance frequencies. It can be shown that at the fourth frequency we have the following field distribution. The field in the cells which are under tuning (cells are marked with a dashed line in Fig. 2) is the superposition of the fields of two $2\pi/3$ travelling waves propagating in opposite directions. The field in the adjusting cells is practically equals to zero. At the first step two identical cells are tuned. Their radii are changed so that the fourth frequency of the cavity stack is equal to $\pi/2$ mode frequency of elementary stack. Then cells are tuned successively [3]. After tuning each ring and each disk has a fixed position in the section.

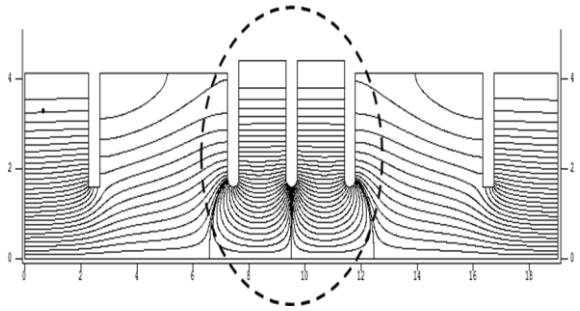

Fig. 2. Field distribution in the π/2 cavity stack for cell tuning (computer code SUPERFISH)

In NSC KIPT brazing of acceleration sections is performed in vertical vacuum furnace with induction heating. The section prepared for brazing is moved in the middle of the annular inductor. Because the maximum value of this moving is limited by the value of 1 m, section is divided into subsections. Each subsection consists of nearly 20 cells.

Silver Braze 72 foil with a thickness of 50 μm is placed between each ring and disk. Using of three guides to align disks and rings by the outer radius, subsection is assembled in the form of the vertical «sandwich». Then with the rod passed through central apertures in the disks, subsection is contracted and loaded into the furnace without guides. Vacuum system consisting of the fore-vacuum, turbomolecular and ion pumps allows obtaining a high vacuum in furnace chamber. Heating temperature is measured with a pyrometer. It is possible to observe visually the melting of the braze. Since the melting point of the braze is well known, this procedure is used for the initial calibration of the pyrometer.

Each subsection is brazed a joint by a joint while mowing inside inductor. Thus all four subsections were brazed.

The details of the couplers (Fig. 3) are tuned and then are brazed in vacuum furnace with electrical heating elements [4]. All the vacuum joints of brazed elements are checked for vacuum integrity on helium leak detector (sensitivity on helium to $7 \cdot 10^{-13}$ m^3P/s, Fig. 4). Then input coupler is brazed to the first subsection in induction furnace.

Second, third, fourth subsections and output coupler are brazed to the first subsection consecutively.

Fig. 3. The details of input (top) and output (bottom) couplers

Fig. 4. Vacuum testing of subsection on helium leak detector

The process of loading of the fourth subsection into the induction vacuum furnace is shown in Fig. 5.

After brazing and testing for vacuum integrity of the whole structure, the section is mounted on the frame and prepared for tuning measuring system.

Fig. 5. Loading of the fourth subsection into the induction vacuum furnace, subsection is in chamber (output coupler is not brazed)

2. MEASURING SYSTEM

The measuring system used for experimental investigation of electrodynamic characteristics of accelerating section is based on the HP 8753C network analyzer (Fig. 6, at the top). This analyzer has integrated synthesized source of microwave power with a step by frequency of 1 Hz in the range from 300 kHz to 3 GHz. Dynamic accuracy of the receiver is not worse than ±0.05 dB by the amplitude and ±0.3° by the phase in the range of the amplitudes more than 50 dB. The analyzer exchanges the measurement data with a personal computer (PC) via the GPIB protocol. Signals from the directional coupler (DC) connected to the accelerating section (AS) are fed to the analyzer. This enables measuring of complex coefficient of wave reflection from the section. Matched load (ML) is placed at the exit of AS. Measuring of reflection coefficient gives the opportunity to investigate a number of section characteristics particularly band pass characteristic, field attenuation, amplitude and phase distribution on the axis.

The system for measuring of the on axis field distribution with the bead-pull techniques [5] was developed. The alumina ceramic tube with the external diameter of 1.8 mm, the internal diameter of ~ 0.5 mm and the length of 5 mm is used as a bead. After the bead calibration in E_{010} cavity we obtain the value of the formfactor k_e=1.06·10^{-19} m^{2}s/Ω. For moving of the bead a stepping motor (SM) with a step of 0.9° and driver which allows the minimum rotation of the motor axis on 1/16 of the step (bead linear displacement depends on the diameter of the shaft on which filament is wound and in our case it is equal to 16 μm) are used.

Driver is controlled by a microcontroller STM32F3 (CSM) via the commands interchange with PC through USB port. The design of developed and fabricated system of bead moving (see Fig. 6, at the bottom) prevents the filament displacement in perpendicular to main moving direction and allows to move the bead over long distances quickly enough. Moreover the fabricated system allows to conduct the measurements only in the centers of the cells, that accelerates the process of section tuning significantly. In general the developed software realizes three operating modes: measuring at a given step of field distribution in the whole section; measuring of the field in the centers of the cells along the whole section or the part of the section; tuning mode, when the fields are measured in the middle of the cell under tuning and fourth adjacent ones.

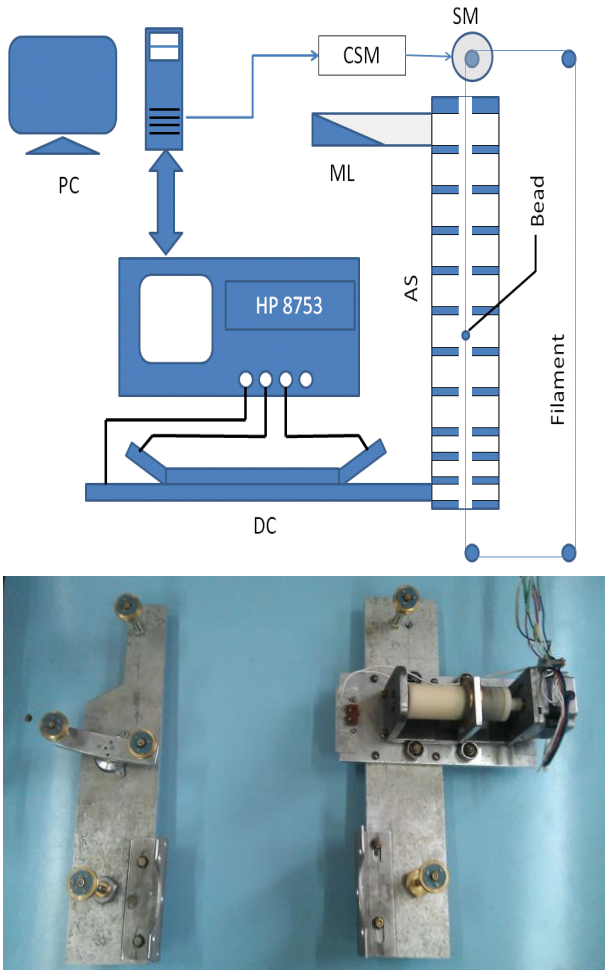

Fig. 6. Layout of measuring system of section characteristics (top) and the system for bead moving (bottom)

It should be noted that measuring of section characteristics is conducted under conditions which are different from operating ones: section is not evacuated and the operating temperature is not supported. So each measurement session is accomplished by frequency recalculation with taking into account the corrections on vacuum and temperature variance [6]. It is assumed that condition of thermal equilibrium between the section and the surrounding space is fulfilled, that is the temperature of the section is equal to the temperature of the air. The problem is in the fact that environmental conditions can arbitrarily vary during the measurement session. To improve the accuracy of the measurement results, the following method of correcting is used. Unperturbed reflection coefficient (bead is beyond the section) is measured at the start and at the end of measuring session. Difference in these values of reflection coefficient indicates a specific changing of the environmental conditions. As we obtain two values of unperturbed reflection coefficient, so we can implement only a linear correction of the results supposing that environmental conditions vary linearly with time. The effect of using of the correction method due to the changing of environmental conditions is shown in Fig. 7.

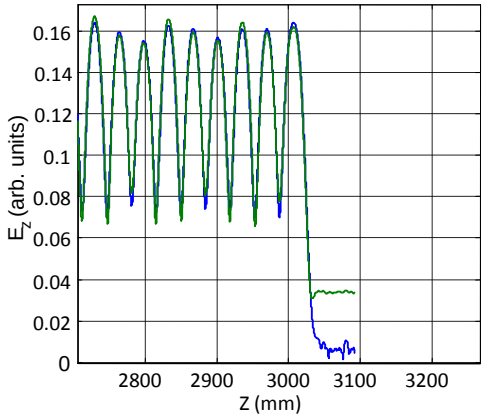

Fig. 7. Field amplitude distribution at the section exit: the method of correcting of environmental conditions is used (blue curve) and it is not used (green curve)

As it is evident from the field amplitude distributions in Fig. 7 (near Z = 3100 mm), mentioned above method increases the measuring range at least by five times.

It is obvious that random errors can have a significant effect on the measurement results. To answer this question, measuring of field distribution in the section was conducted repeatedly. Results are shown in Fig. 8. At the exit of the section errors are less than errors at the section entrance due to increasing of the field. Respectively, in the initial part of the section the errors are more considerable. Repeatability of measurement results of field amplitude and phase is fairly good. In the main part of the section relative rms deviation of the amplitude (4σ) does not exceed ±1%, and rms deviation of the phase is less than (4σ) ±1°.

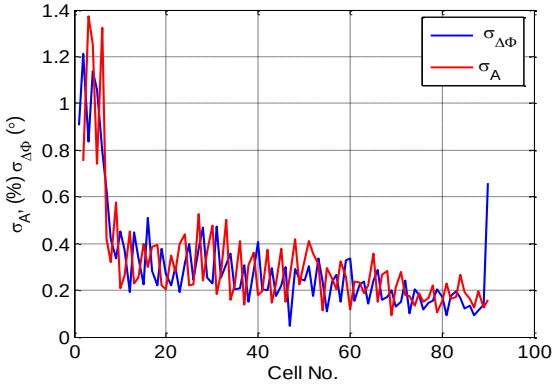

Fig. 8. Rms spread of amplitude and phase of the field in the section cells from six measurements

Therefore one can conclude that the measuring system used for the investigation of accelerating section electrodynamic characteristics provides high reliability of the experimental data.

3. TUNING AND EXPERIMENTAL RESULTS

The developed tuning technique is based on some modification of the approaches outlined in [7 - 12]. To tune the cell, the structure on axis complex fields are determined in three consecutive cells (cell under tuning and two adjacent ones). The following expression is used:

$$S = \frac{E_c(z-D)+E_c(z+D)}{2E_c(z)}, \qquad (1)$$

where D is the distance between the centers of the adjacent cells, $E_c(z)$ is the on axis complex field at the point with coordinate z.

Let's consider the Eq. (1). In tuned periodic structure field amplitudes in all cells are equal, $|E_c(z-D)| = |E_c(z)| = |E_c(z+D)|$, and phase shift per cell is constant, $\arg(E_c(z)) - \arg(E_c(z-D)) = \arg(E_c(z+D)) - \arg(E_c(z)) = \Phi$. In this case we have $S \equiv \cos\Phi$. Suppose, that field amplitude distribution in tuned inhomogeneous structure has the form $|E_c(z-D)| = |E_c(z)| - \delta$ and $|E_c(z+D)| = |E_c(z)| + \tilde{\delta}$, where $\delta, \tilde{\delta} > 0$ corresponds to the increasing field distribution and $\delta, \tilde{\delta} < 0$ to the decreasing one. At the operating frequency phase shift per cell is constant, Φ. Then we obtain

$$S = \cos\Phi\left(1 + \frac{\tilde{\delta}-\delta}{2|E_c(z)|}\right) + i\sin\Phi\,\frac{\tilde{\delta}+\delta}{2|E_c(z)|}. \qquad (2)$$

In this case S has a complex value. However if the field amplitudes change evenly, $\delta = \tilde{\delta}$, and weakly, $\delta/|E_c(z)| \ll 1$, the following conditions are fulfilled: the real part of S Re(S) = cosΦ and the imaginary part of S Im(S) $\ll 1$. In this case for 2π/3 section a criterion of tuning is Re(S) $\Rightarrow$ –0.5 but if $\delta \neq \tilde{\delta}$ the condition Re(S) = –0.5 does not correspond to Φ = 2π/3.

It should be noted that analysis of section tuning is resulted in more depth investigation of the problems of inhomogeneous section tuning [13 - 15].

Field distribution in the untuned section at the operating frequency is shown in Fig. 9. Despite the preliminary tuning of the cells, there are reflections in different parts of the section. It should be noted that phase advance per cell is negative because we measure the reflected wave that propagates in opposite to accelerating wave direction. The largest deviations of phase advance per i^{th} section cell from -120° ($\Delta\Phi = \Phi_{i+1} - \Phi_i + 120°$) are observed in the couplers. These deviations are expected since couplers are not the section regular cells.

Tuning of the section is achieved in several stages. After the preliminary tuning of the cells (π/2 cavity stack) the cell rings have been slightly oversized assuming possibility to rise its frequencies by some deformations of the sidewalls through special bore recess (see the ring sidewalls in Fig. 1 and Fig. 3). At the first tuning stage the frequency with the closest approach of average phase shift per cell to -120° has been determined. In our case this frequency is 2855 MHz. At this frequency the dependence of S on the cell number is maximally aligned. For the adjacent cells with values of S highly differ in opposite directions from -0.5 that values are corrected by disk deflection. Disk is deflected towards the cell with Re(S) > -0.5. Further the internal wall of the cell with Re(S) < -0.5 is deformed so that Re(S) = -0.5±0.005. At the following stages of tuning last procedure is repeated for several frequencies (with a

step about of 300 kHz) until the operating frequency is reached. Field distribution in the section after tuning is shown in Fig. 10.

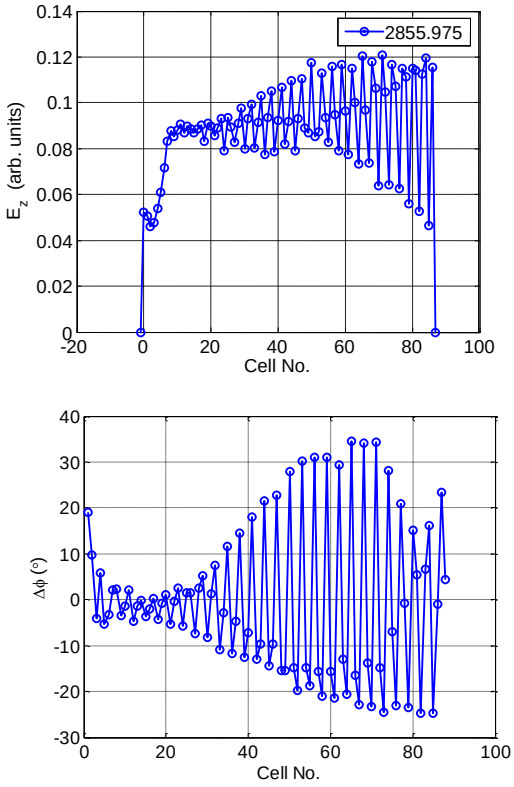

Fig. 9. Field distribution in the section before tuning

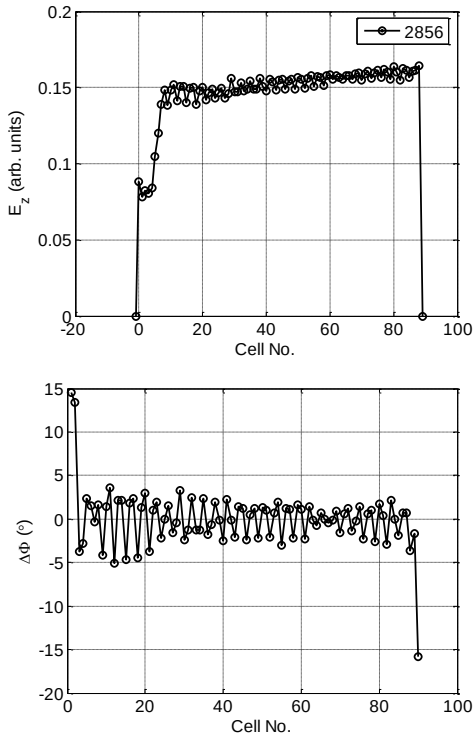

Fig. 10. Field distribution in the section after tuning

At developing travelling wave accelerating sections one of the most important problems is the accordance of really obtained characteristics with simulated ones. Especially it concerns sections with large inhomogeneity. It is seen in Fig. 11 that the measured and calculated on axis field amplitudes coincide well enough in the beginning of the section. Power of microwave supply is P_0=4.6 MW in the experiment and simulation. The maximum difference of the field amplitudes is 9.4% in the seventh cell. The difference is well within that value for the whole section.

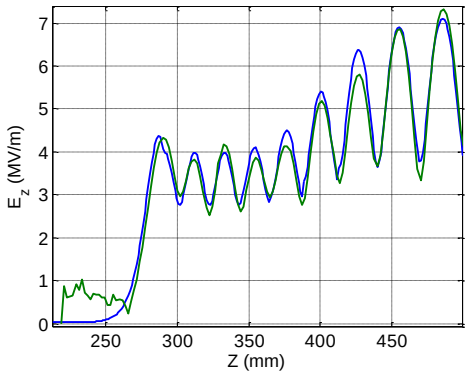

Fig. 11. On axis field amplitude distribution in the initial part of the section: experiment (green curve) and simulation (blue curve)

The voltage standing wave ratio (VSWR) in the frequency range 2853…2858 MHz is shown in Fig. 12. According to the technical specifications of the klystron the VSWR values should not exceed 1.5 that is performed in our case.

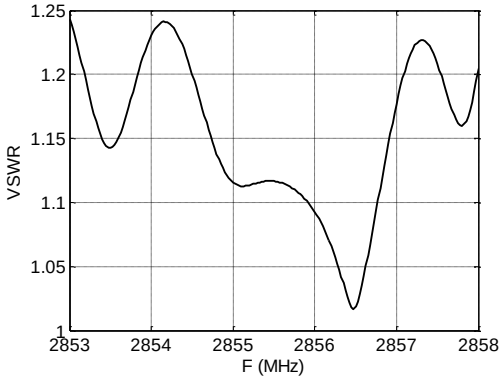

Fig. 12. Bandpass characteristic of the section near the operating frequency 2856 MHz

The value of group velocity has theoretical and practical significance. The specific value of group velocity substantiates the credibility of mathematical models used for simulation of inhomogeneous section. In practice the value of group velocity results in restrictions concerned with the pulse regime operation. Almost all the filling time of the section that depends on the group velocity falls out of useful operating time because of large energy spread of electrons. Furthermore too short rise time of the RF pulse as compared to section filling time can results in waveguide breakdowns.

As well known the relative group velocity β_g is defined as the derivative of the dispersion curve: $\beta_g = v_g/c$, $v_g = d\omega/dk$, where c is the velocity of light, ω is the circular frequency, k is the wave number. It can be shown that $\beta_g = 120^\circ \cdot \Delta F / F_0 \, \Delta\Psi^\circ$, where ΔF is the linear frequency band around the operating frequency F_0, $\Delta\Psi^\circ$ is the deviation of phase advance averaged over section cells from 120° in the corresponding frequency band ΔF. Measuring the field distribu-

ISSN 1562-6016. ВАНТ. 2016. №3(103)

tion in the section, we have obtained the required dependence that is shown in Fig. 13. Phase shifts in couplers and adjacent cells are not counted since the fields in these cavities are perturbed by section ends. We obtain the following value of average group velocity $\beta_g = -2.67\,\%$. It is negative because we measure the reflected wave that propagates in opposite to accelerating wave direction as it was mentioned above.

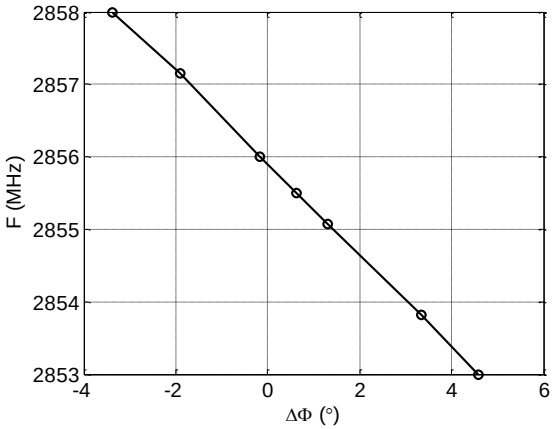

Puc. 13. Dispersion curve near the operating frequency

Knowing the group velocity one can obtain the filling time: $L/v_g = 366$ ns, where L is the section length, which is considered when Fig. 13 is plotted.

Attenuation is another one important characteristic of the section. There is known procedure measuring attenuation of a two-port network. A movable shorting plunger is connected to the second port while return losses S_{11} is measured at the firs port. Because of imperfection matching of the network and network analyzer S_{11} varies with the plunger moving due to resonance properties of the network. To diminish such measurement errors S_{11} is arithmetic mean between those maximal and minimal values and attenuation is a half of S_{11} because the wave attenuates twice. Due to design features of the section output waveguide it is inconvenient to replace the matched load with the movable shorting plunger at this stage of section manufacturing. Thus we put the plunger in the output coupler. Dependence of S_{11} on the frequency is shown in Fig. 14. There are a local maximum of reflection at the operating frequency and two local minimums of reflection nearby. The average value between the local maximum and the left local minimum is -4.65 dB. The average value between the local maximum and the right local minimum is -4.53 dB. Similarly with the above one can estimate the following values of attenuation: 0.261 Np and 0.269 Np, accordingly. The average of these values of 0.264 Np is good choice for estimated attenuation. The calculated value of attenuation is 0.247 Np [1], so the difference between the measured and calculated value is 6.7%. Such correspondence is very good.

Measured and calculated values of section parameters are contained in Table. Comparing the values in second and third columns of Table, one can conclude that measurement results are in good agreement with calculated ones.

The photo of the section after measurements is shown in Fig. 15. Presently the section is under vacuum and is ready to be installed on the frame of the linac.

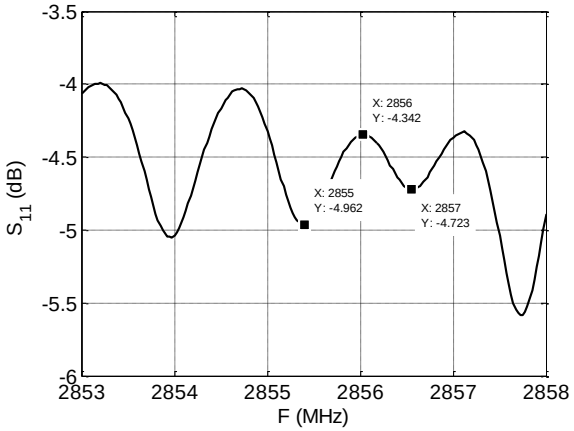

Fig. 14. Dependence of reflection coefficient vs frequency when plunger is in the output coupler

Characteristics of accelerating section

Parameter	Measured	Simulated
Operating frequency, MHz	2856	2856
Operating temperature, degr,°C	40	40
Average phase shift per cell, degr.	120	120
The rms deviation of phase advance from 120°, degr.	2	–
VSWR at the operating frequency	1.09	<1.01
VSWR in the frequency band 2853…2858 MHz	<1.25	<1.1
Total length, m	3.105	3.105
Filling time, ns	366	385
Attenuation, Np	0.261	0.247

Fig. 15. Photo of the section on the frame (section is under vacuum)

CONCLUSIONS

The accelerating section of the electron linac with the energy to 10 MeV and average beam power to 20 kW has been fabricated. Electrodynamic characteristics of the section were investigated experimentally. It was shown that measurement results are in good agreement with calculated ones. The developed and fabricated accelerating section satisfies specifications of the linac designed.

REFERENCES

1. M.I. Ayzatskiy, A.N. Dovbnya, et al. Accelerating system for an industrial linac // *Problems of Atomic Science and Technology. Series "Nuclear Physics Investigations"*. 2012, № 4, p. 24-28.
2. V.F. Zhiglo, V.A. Kushnir, et al. Cooling system for the LU-10 accelerating section // *Problems of Atomic Science and Technology. Series "Nuclear Physics Investigations"*. 2015, № 6, p. 18-22.
3. M.I. Ayzatsky, E.Z. Biller. Development of inhomogeneous disk-loaded accelerating waveguides and rf-coupling // *Proc. of Linear Accelerator Conf.* 1996, p. 119-121.
4. N.I. Aizatskyi, K.Yu. Kramarenko, et al. On a method of tuning of couplers for electron linacs based on disk loaded waveguides // *Problems of Atomic Science and Technology. Series "Nuclear Physics Investigations"*. 2015, № 6, p. 8-12.
5. Charles W. Steele. A nonresonant perturbation theory // *IEEE Trans. on microwave theory and techniques*. 1966, v. 14, № 2, p. 70-74.
6. *Handbook of the electrotechnical materials* / Edited by K.A. Andrianova, et al. M.-L.: GEI, 1958, v. 1.
7. T. Khabiboulline, V. Puntus, et al. A new tuning method for travelling wave structures // *Proc. of Particle Accelerator Conf.* 1995, p. 1666-1668.
8. J. Shi, A. Grudiev, et al. Tuning of CLIC Accelerating Structure Prototypes at CERN // *Proc. of Linear Accelerator Conf.* 2010, p. 97-99.
9. N.M. Kroll, C.-K. Ng, D.C. Vier. Applications of time domain simulation to coupler design for periodic structures // *Proc. of Linear Accelerator Conf.* 2000, p. 614-617.
10. W.C. Fang, Z.T. Zhao, et al. R&D of C-band accelerating structure at SINAP // *Proc. of Linear Accelerator Conf.* 2010, p. 199-201.
11. D Alesini, A Citterioc, et al. Tuning procedure for traveling wave structures and its application to the C-Band cavities for SPARC photo injector energy upgrade // *Journal of Instrumentation*. 2013, v. 8, p. 1-18.
12. W.C. Fang, Q. Gu, et al. The nonresonant perturbation theory based field measurement and tuning of a linac accelerating structure // *Proc. of Linear Accelerator Conf.* 2012, p. 375-375.
13. M.I. Ayzatsky, V.V. Mytrochenko. *Electromagnetic fields in nonuniform disk-loaded waveguide*. ArXiv:1503.05006 [physics.acc-ph]. 2015, 19 p.
14. M.I. Ayzatsky, V.V. Mytrochenko. *Coupled cavity model based on the mode matching technique*. ArXiv:1505.03223 [physics.acc-ph]. 2015, 12 p.
15. M.I. Ayzatsky, V.V. Mytrochenko. *Coupled cavity model for disc-loaded waveguides*. ArXiv: 1511.03093 [physics.acc-ph]. 2015, 26 p.

Article received 03.03.2016

УСКОРЯЮЩАЯ СЕКЦИЯ ТЕХНОЛОГИЧЕСКОГО ЛИНЕЙНОГО УСКОРИТЕЛЯ ЭЛЕКТРОНОВ

Н.И. Айзацкий, Е.З. Биллер, А.Н. Довбня, Е.Ю. Крамаренко, И.В. Ходак, В.А. Кушнир, В.В. Митроченко, Т.Ф. Никитина, А.Н. Опанасенко, С.А. Пережогин, Д.Л. Стёпин, Л.И. Селиванов, В.Ф. Жигло

Приведены параметры конструкции и результаты исследования электродинамических характеристик ускоряющей секции с набегом фазы 120° на рабочей частоте 2856 МГц, предназначенной для модернизации ускорителя электронов ЛУ-10 ННЦ ХФТИ. Полученные экспериментальные данные сравниваются с расчётными.

ПРИСКОРЮВАЛЬНА СЕКЦІЯ ДЛЯ ТЕХНОЛОГІЧНОГО ЛІНІЙНОГО ПРИСКОРЮВАЧА ЕЛЕКТРОНІВ

М.І. Айзацький, Є.З. Біллер, А.М. Довбня, К.Ю. Крамаренко, І.В. Ходак, В.А. Кушнір, В.В. Митроченко, Т.Ф. Нікіміна, А.М. Опанасенко, С.А. Пережогін, Д.Л. Стьопін, Л.І. Селіванов, В.Ф. Жигло

Наведено параметри конструкції і результати дослідження електродинамічних характеристик прискорювальної секції з набігом фази 120° на робочій частоті 2856 МГц, яка призначена для модернізації прискорювача електронів ЛУ-10 ННЦ ХФТІ. Отримано експериментальні дані, які порівнюються з розрахунковими.